Research Square

Preprints are preliminary reports that have not undergone peer review.
They should not be considered conclusive, used to inform clinical practice,
or referenced by the media as validated information.

Symmetry Breaking and Spatio-temporal Pattern Formation in Tumor Growth: A Fast-Slow Reaction-Diffusion Approach

Grace Kim
Arizona State University
Dongyung Kim
dongyungkim@gmail.com
Benedictine University

Research Article

Keywords: Symmetry breaking, Tumor growth,Turing Instability, Fast-slow dynamics, Reaction-diffusion system

Posted Date: May 26th, 2026

DOI: https://doi.org/10.21203/rs.3.rs-9794776/v1

License: This work is licensed under a Creative Commons Attribution 4.0 International License.
Read Full License

Additional Declarations: No competing interests reported.

Symmetry Breaking and Spatio-temporal Pattern Formation in Tumor Growth: A Fast-Slow Reaction-Diffusion Approach

GRACE KIM[1,*] **and DONGYUNG KIM**[2,**]

[1]Department of Biological Sciences (Biomedical Sciences), Arizona State University, Tempe, AZ, USA
[2]Department of Mathematical and Computational Sciences, Benedictine University (BenU), Lisle, IL and Mesa, AZ, USA
[*]gkim99@asu.edu,applecube11@gmail.com
[**]corresponding to Dongyung Kim: dkim@ben.edu, dongyungkim@gmail.com,
https://orcid.org/0000-0003-4628-6895

ABSTRACT

This study explores the emergence of complex spatial architectures in tumor progression through the lens of symmetry breaking and non-equilibrium dynamics. Using a singularly perturbed reaction-diffusion framework, we demonstrate that the interplay between cellular kinetics and nutrient transport leads to *Turing-type instabilities*, which serve as the primary mechanism for spatio-temporal pattern formation. By applying a *fast-slow dynamics* approach, we analytically characterize the transition from uniform states to heterogeneous growth, highlighting how disparate time scales between metabolic reactions and spatial diffusion drive the evolution of tumor morphology. Our findings reveal that the resulting spatial heterogeneity is not merely stochastic but a predictable consequence of biophysical instabilities. These results provide a robust theoretical basis for understanding the irregular boundaries and multi-focal growth patterns observed in clinical imaging, offering new insights into the physical constraints of tumor invasiveness.

Keywords: Symmetry breaking, Tumor growth,Turing Instability, Fast-slow dynamics, Reaction-diffusion system

1 Introduction

Previous research investigated cancer through image segmentation[1]. This segmentation allows for the precise detection of tumor regions from the whole image. Furthermore, it is necessary to develop cancer tumor growth nonlinear dynamical system models. Recent studies in this journal have highlighted the significance of self-organized pattern formation in reaction-diffusion systems[2]. Specifically, the role of diffusive instability in three-species cancer models has demonstrated how spatial heterogeneity drives tumor expansion[3]. The mathematical modeling of tumor growth has become a fundamental tool in oncology, providing predictive insights into disease progression and assisting in the optimization of therapeutic strategies. While classical models, such as the Logistic and Gompertz equations, have successfully captured the macroscopic growth rates of total tumor burden[4,5], they often rely on the assumption of spatial homogeneity. However, clinical evidence increasingly indicates that tumor progression is inherently a spatial process, driven by significant intra-tumor heterogeneity and the complex interplay between different cell subpopulations. The primary research question of this study is to investigate how the spatial interaction between proliferating cancer cells (P) and quiescent cells (Q) dictates the overall expansion and stability of a tumor. In a realistic biological microenvironment, cancer cells are not stationary; they exhibit **random motility** as they invade surrounding healthy tissues to seek nutrients or escape metabolic stress. We represent this movement using **Laplacian diffusion terms**, $\nabla^2 P$ and $\nabla^2 Q$, which mathematically describe the net flux of cell populations according to Fick's law. This allows the model to transition from a purely temporal view to a spatio-temporal framework, capturing the non-uniform expansion of the tumor boundary and the emergence of spatial patterns. A recurring challenge in mathematical oncology is the trade-off between biological complexity and computational or analytical clarity. In this paper, we focus on a **one-dimensional (1D) spatial domain** to investigate these dynamics. This simplification is a deliberate choice intended to isolate the fundamental mechanisms of the "fast-slow" interaction between P and Q cells and to observe how differential diffusion coefficients ($d_P \neq d_Q$) trigger symmetry-breaking instabilities. This 1D analysis serves as a critical theoretical baseline and a necessary step before extending the model to more complex 2D or 3D geometries. Building upon ratio-dependent growth models and the Michaelis-Menten functional response, we propose a nonlinear dynamical system that incorporates a density-dependent mortality function for quiescent cells. Our model accounts for the biological reality where the death of quiescent cells is accelerated by metabolic

competition or signaling interference from the proliferating population. Through this framework, we explore the conditions under which spatial heterogeneity leads to persistent oscillations or steady-state patterns, providing a mathematical basis for the intermittent growth patterns often observed in clinical settings. The primary research question of this study investigates how the spatial interaction between proliferating cells (P) and quiescent cells (Q) dictates overall expansion and stability. A critical feature of our model is the identification of a **singularly perturbed structure**. By defining ε as the ratio between cell transition rates and proliferation rates, we isolate the *fast-slow dynamics* that govern the system's evolution. This time-scale separation allows for the emergence of relaxation oscillations, mirroring the intermittent growth and dormant phases frequently documented in clinical oncology. Furthermore, we address the role of **diffusion-driven instability** (Turing instability) in symmetry-breaking. In a realistic biological microenvironment, cancer cells exhibit random motility represented by Laplacian operators $\nabla^2 P$ and $\nabla^2 Q$. We show that the interplay between these motility terms and the Michaelis-Menten type functional response leads to the formation of complex spatial patterns. This transition from purely temporal kinetics to a spatio-temporal framework is essential for predicting the invasive potential of solid tumors. Building upon the rich tradition of nonlinear modeling published in this journal, our study contributes to the mathematical understanding of complex biological systems. We provide a rigorous evaluation of the conditions under which spatial heterogeneity leads to persistent oscillations, offering a theoretical baseline for drug selection and therapeutic design.

1.1 Revisiting Classical Foundations in a Spatial Context

The trajectory of mathematical oncology has long been anchored in deterministic growth laws that characterize the temporal expansion of tumor volume. Historically, the **Logistic growth model** and the **Gompertz equation** have served as the fundamental benchmarks for quantifying neoplastic populations[4,5]. While the Logistic framework assumes a growth rate that diminishes linearly as the population approaches a carrying capacity K, the Gompertzian approach accounts for an exponentially decaying proliferation rate, mirroring the clinical observation that tumor expansion decelerates as the total mass increases. From a mechanistic perspective, these established frameworks can be reformulated as a dynamic partitioning of the total cell count N into functionally distinct states. Following the conceptual lineage of Gyllenberg and Webb[5], we consider a biological system where cells undergo transitions between an active proliferating state (G) and a non-replicative quiescent state (R). This state-switching is typically represented as a density-dependent process, where the likelihood of a cell entering dormancy is a function of the cumulative tumor burden $r(N)$. By integrating these individual state dynamics, the macroscopic growth of the malignancy is governed by:

$$\begin{aligned} \frac{dG}{dt} &= cG - \Gamma(N)G, \\ \frac{dR}{dt} &= \Gamma(N)G \end{aligned} \tag{1.1}$$

where the total population $N = G + R$ is fundamentally driven by the mitotic flux of the G fraction.

However, these purely temporal approximations often fall short of capturing the **intra-tumor spatial heterogeneity** that defines aggressive clinical cases. A solid tumor is not a homogeneous suspension of cells; rather, it is a highly structured entity where peripheral cells exhibit distinct kinetic behaviors compared to those in the core due to nutrient scarcity and mechanical stress. To address this limitation, our study transcends these classical ODE-based foundations by embedding **Laplacian diffusion operators**. This extension allows for the local migration of cells, evolving the system into a rigorous spatio-temporal reaction-diffusion framework that accounts for the non-uniform distribution and invasive potential of the tumor. Denote by $P(t)$ the population densities of the proliferating cancer cells, $Q(t)$ the population densities of the remains quiescent the at time t and N tumor burden. Then the ratio-dependent type tumor growth model with Michaelis-Menten type functional response is given as follows:

$$\frac{dP}{dt} = rP\left(1 - \frac{P}{K}\right) - \frac{aPQ}{mQ+P}, \tag{1.2a}$$

$$\frac{dQ}{dt} = Q\left[-r(Q) + \frac{bP}{mQ+P}\right], \tag{1.2b}$$

$$N = P + Q \tag{1.2c}$$

where a, b, m, K, and r are positive constants. In (1.2), $r(Q)$ denotes a death rate function of quiescent cell, and r the cancer cell growth rate with intrinsic growth rate and K carrying capacity in the absence of death cell, respectively, while a, b, and m are model-dependent parameter constants.

According to Stochastic Model of Intra-Tumor Heterogeneity (SMITH)[6], tumor cells exhibit spatial heterogeneity. It is evident that tumor cells do not proliferate uniformly. As established by SMITH[6], tumor progression is fundamentally

characterized by spatial heterogeneity. To capture this complex phenomenon, our study extends traditional dynamical systems by integrating spatial nonuniform components, thereby accounting for the non-uniform distribution and migration of cell populations within the tissue. Consequently, we move beyond spatially homogeneous models by appending Laplacian diffusion terms to the governing equations, allowing for a more rigorous analysis of spatial-temporal tumor dynamics. Furthermore, we investigate the influence of diffusion across various modeling frameworks with stability[7–14].

We add *Laplacian* diffusion terms to the current tumor growth models.

$$\begin{aligned}
\frac{\partial P}{\partial t} &= rP\left(1-\frac{P}{K}\right)-\frac{aPQ}{c+P}+D_P\frac{\partial^2 P}{\partial x^2}, \quad x\in(0,l), t>0, && \text{(1.3a)}\\
\frac{\partial Q}{\partial t} &= Q\left[-r(Q)+\frac{bP}{c+P}\right]+D_Q\frac{\partial^2 Q}{\partial x^2}, \quad x\in(0,l), t>0, && \text{(1.3b)}\\
N &= P+Q && \text{(1.3c)}
\end{aligned}$$

where the specific death rate of the quiescent cell is given by

$$r(Q)=\frac{\rho+\sigma P}{1+P}, \tag{1.4}$$

which depends on the quantity of quiescent cell. The spedific death rate function $r(Q)$ represents a density-dependent mortality. Unlike constant death rates, this formulation captures the biological reality where the death of quiescent cells is accelerated by the metabolic competition or signaling interference from the proliferating cell population P. Here, the positive constants ρ and σ denote the minimal death rate and the limiting death rate of the cancer, respectively. Throughout the paper, the following natural condition

$$0<\rho\leq\sigma \tag{1.5}$$

will be assumed, and we will consider the case of the constant diffusivity, $D_P, D_Q > 0$. The advantage of this model is that the cancer death rate is neither a constant nor an unbounded function, but still it is increasing with the cancer cell abundance. On the other hand, combining (1.1) and (1.3), many authors (see[13,15,16], for instance) have studied a more general model as follows:

$$\begin{aligned}
\frac{\partial P}{\partial t} &= rP\left(1-\frac{P}{K}\right)(-\frac{aPQ}{mQ+P}+D_P\frac{\partial^2 P}{\partial x^2}, \quad x\in(0,l), t>0, && \text{(1.6a)}\\
\frac{\partial Q}{\partial t} &= Q\left[-r(Q)+\frac{bP}{mQ+P}\right]+D_Q\frac{\partial^2 Q}{\partial x^2}, \quad x\in(0,l), t>0, && \text{(1.6b)}\\
N &= P+Q && \text{(1.6c)}
\end{aligned}$$

with the specific death rate of the cancer somewhat restricted in the form

$$r(Q)=d. \tag{1.7}$$

In this paper we consider a ratio-dependent reaction-nonuniform cancer cell-quiescent cell model with Michaelis-Menten type functional response and the specific death rate of the cancer given by (1.4) instead of (1.7). We study the effect of the spatial nonuniform term on the stability of the stationary solutions. Also we explore under which parameter values instability can occur giving rise to non-uniform stationary solutions satisfying the following equations:

$$\begin{aligned}
\frac{\partial P}{\partial t} &= rP\left(1-\frac{P}{K}\right)-\frac{aPQ}{mQ+P}+D_P\frac{\partial^2 P}{\partial x^2}, \quad x\in(0,l), t>0, && \text{(1.8a)}\\
\frac{\partial Q}{\partial t} &= Q\left[\frac{bP}{mQ+P}-\frac{\rho+\sigma Q}{1+Q}+\right]+D_Q\frac{\partial^2 Q}{\partial x^2}, \quad x\in(0,l), t>0, && \text{(1.8b)}\\
N &= P+Q && \text{(1.8c)}
\end{aligned}$$

assuming that cancer cell and quiescent cell are diffusing according to Fick's law in the interval $x\in[0,l]$. We are interested in the solutions $P,Q:(l,0)\times\mathbb{R}^+\to\mathbb{R}^+$ fulfilling the Neumann boundary conditions

$$Q_x(0,t)=Q_x(l,t)=Q_x(0,t)=Q_x(l,t)=0, \tag{1.9}$$

and initial conditions

$$P(x,0)\geq 0, \quad Q(x,0)\geq 0, \quad x\in(0,l).$$

1.2 Nondimensionalization and Parametric Scaling

To enhance the analytical tractability of the system and reduce the number of independent parameters, we apply a nondimensionalization procedure. This process allows us to identify the fundamental scales governing the tumor dynamics and simplifies the comparison between distinct biological mechanisms. We introduce the following dimensionless variables for time, space, and cell densities:

$$\bar{P} = \frac{P}{K}, \quad \bar{Q} = \frac{Q}{K}, \quad \bar{t} = ct, \quad \bar{x} = \frac{x}{L}. \tag{1.10}$$

By rescaling the populations P and Q relative to the carrying capacity K and normalizing the time scale by the proliferation rate c, we transform the original system into a dimensionless framework. Substituting these variables into the governing equations yields a set of simplified parameters that represent the relative strengths of biological processes:

$$\begin{aligned} \varepsilon = \frac{k}{c}, \quad \alpha = \frac{a}{c}, \quad \rho = \frac{d}{k}, \quad \beta = Kb, \quad \sigma = \frac{f}{k}, \\ d_{\bar{P}} = \frac{d_P}{cL^2}, \quad d_{\bar{Q}} = \frac{d_Q}{cL^2}. \end{aligned} \tag{1.11}$$

Here, ε represents the ratio between the transition rate of quiescent cells and the growth rate of proliferating cells, while α quantifies the inhibitory coupling effect normalized by the growth rate. The coefficients $d_{\bar{P}}$ and $d_{\bar{Q}}$ now characterize the dimensionless motility of the respective populations relative to the spatial domain size L.

Under this scaling, and omitting the bars for notational simplicity, the spatio-temporal dynamics are governed by:

$$\begin{cases} \dfrac{\partial P}{\partial t} = P(1-P) - \dfrac{\alpha PQ}{Q+P} + d_P \dfrac{\partial^2 P}{\partial x^2}, \\ \dfrac{\partial Q}{\partial t} = \varepsilon Q \left[-\dfrac{\rho + \sigma\beta Q}{1+\beta Q} + \dfrac{P}{Q+P} \right] + d_Q \dfrac{\partial^2 Q}{\partial x^2}. \end{cases} \tag{1.12}$$

This dimensionless form reveals that the system is a **singularly perturbed reaction-diffusion system** when $\varepsilon \ll 1$, emphasizing the separation of time scales between the rapid proliferation phase and the slower metabolic shifts in the quiescent sub-population.

Specifically, the differential diffusion rates ($d_P \neq d_Q$) model the spatial heterogeneity of tumor, where proliferating cells may invade surrounding tissues more aggressively than quiescent cells. This spatial coupling is essential for predicting the non-uniform expansion of tumor boundary.

Conveniently, we consider $N = P + Q$ later. First, set

$$\mathbf{F} = \begin{pmatrix} F_1 \\ F_2 \end{pmatrix}, \mathbf{u} := \begin{pmatrix} P \\ Q \end{pmatrix} D := \begin{pmatrix} d_P & 0 \\ 0 & d_Q \end{pmatrix},$$

where

$$F_1(P,Q) = P(1-P) - \frac{\alpha PQ}{Q+P}, \quad F_2(P,Q) = \varepsilon Q \left[-\frac{\rho + \sigma\beta Q}{1+\beta Q} + \frac{P}{Q+P} \right].$$

$$\begin{pmatrix} P \\ Q \end{pmatrix}_t = \begin{pmatrix} F_1(P,Q) \\ F_2(P,Q) \end{pmatrix} + D \frac{\partial^2 \mathbf{u}}{\partial x^2}$$

Then the system (1.12) with the boundary conditions (1.9) takes the form

$$\mathbf{u}_t = \mathbf{F}(\mathbf{u}) + D \frac{\partial^2 \mathbf{u}}{\partial x^2}; \quad \mathbf{u}_x(0,t) = \mathbf{u}_x(l,t) = \mathbf{0}. \tag{1.13}$$

Clearly, in case P and Q are spatially homogeneous, the spatially constant solution $\mathbf{u}(t) = (P(t), Q(t))^T$ of (1.13), fulfilling the boundary conditions obviously, satisfies the kinetic system

$$\mathbf{u}_t = \mathbf{F}(\mathbf{u}). \tag{1.14}$$

2 Kinetics of the Non-Spatial Tumor Model

In this section, we investigate the underlying dynamical behavior of the system (1.12) by assuming a spatially uniform distribution. By isolating the temporal components, the interaction between proliferating and quiescent cell populations is governed by the following coupled nonlinear ODEs:

$$\begin{aligned}\frac{dP}{dt} &= P(1-P) - \frac{\alpha PQ}{Q+P},\\ \frac{dQ}{dt} &= \varepsilon Q\left[-\frac{\rho+\sigma\beta Q}{1+\beta Q} + \frac{P}{Q+P}\right].\end{aligned} \tag{2.15}$$

The framework in (1.12)(a) introduces a logistic growth mechanism for the P sub-population, representing its expansion towards a normalized carrying capacity. The term $\frac{\alpha PQ}{Q+P}$ characterizes a ratio-dependent functional response, where the parameter α serves as a critical coupling coefficient that quantifies the inhibitory interaction between states.

Regarding the quiescent population, the dynamics in ((2.15)) are governed by a population-type structure scaled by the time-scale parameter ε. Here, the mortality function $\frac{\rho+\sigma\beta Q}{1+\beta Q}$ represents a saturating death rate that evolves from a basal level ρ toward a limiting value σ as the quiescent density increases. By identifying ε as a small positive constant ($0<\varepsilon\ll 1$), the system can be rigorously treated as a **singularly perturbed model**, which explains the rapid adjustment of P relative to the gradual shifts in Q.

If I give an example, often small ε means slower dynamics. Growth term, $\frac{\rho+\sigma\beta Q}{1+\beta Q}$ is a saturating function of Q. As $Q\to 0$, $\frac{\rho+\sigma\beta Q}{1+\beta Q} :\approx \rho$. As $Q\to\infty$, $\frac{\rho+\sigma\beta Q}{1+\beta Q} :\to \sigma$. $\frac{P}{Q+P}$ is loss term because of the interaction. In particular, we will focus on the existence of equilibria and their local stability. In P null-cline, $\frac{dP}{dt} = P(1-P) - \frac{\alpha PQ}{Q+P} = 0$ is either $P=0$ or $1-P = \frac{\alpha Q}{Q+P}$. In Q null-cline, $Q=0$ or $\frac{\rho+\sigma\beta Q}{1+\beta Q} = \frac{P}{Q+P}$. The intersections give equilibria. There are three type of possible equilibrium points. Extinction is $(P,Q)=(0,0)$, Boundary equilibria is $(P,Q)=(1,0)$ and Interior equilibrium is $P^*>0$, and $Q^*>0$. They are obtained by solving the two nullcline equations. ε is time-scale parameter. If $0<\varepsilon\ll 1$, P evolves fast and Q evolves slow. This make the system a slow-fast dynamical system. In the limit $0<\varepsilon\ll 1$, the system (2.15) behaves as a singularly perturbed model. The rapid adjustment of proliferating cells P relative to the slower dynamics of quiescent cells Q leads to relaxation oscillations. This mathematical phenomenon is consistent with clinical observations of intermittent tumor growth, where periods of rapid expansion are followed by dormant phases. The equilibria occur when $\frac{dP}{dt}=0$, $\frac{dQ}{dt}=0$. The equilibria of the system (2.15) are given by the solution of the following equations

$$\frac{dP}{dt} = P(1-P) - \frac{\alpha PQ}{Q+P} = 0, \quad \frac{dQ}{dt} = \varepsilon P\left(-\frac{\rho+\sigma\beta P}{1+\beta Q} + \frac{P}{Q+P}\right) = 0.$$

The system has at least one equilibrium with positive values. This is the point of intersection of P null-cline

$$Q = H_1(P) = \frac{(1-P)P}{\alpha-(1-P)}$$

and Q null-cline

$$Q = H_2(P) = \frac{\rho-\beta(1-\sigma)P+2\sqrt{\{\rho-\beta(1-\sigma)P\}^2-4\beta\delta(1-\rho)P}}{2\beta\delta}.$$

Thus, denoting the coordinates of a positive equilibrium by $(\overline{P},\overline{Q})$, these coordinates satisfy $\overline{Q}=H_1(\overline{P})=H_2(\overline{P})$.

The Jacobian matrix of the system (2.15) linearized at $(\overline{P},\overline{Q})$ is

$$A = \begin{pmatrix} \Phi_1 & -\Phi_2 \\ \Phi_3 & -\Phi_4 \end{pmatrix}, \tag{2.16}$$

where

$$\text{trace}A = \Phi_1 - \Phi_4, \det A = \Phi_2\Phi_3 - \Phi_1\Phi_4$$

and

$$\begin{aligned}\Phi_1 &= -\overline{P} + \frac{\alpha\overline{P}\,\overline{Q}}{(\overline{Q}+\overline{P})^2}, \quad \Phi_2 = \frac{\alpha\overline{P}^2}{(\overline{Q}+\overline{P})^2},\\ \Phi_3 &= \frac{\varepsilon\overline{Q}^2}{(\overline{Q}+\overline{P})^2}, \quad \Phi_4 = \frac{\varepsilon\beta\overline{Q}(\sigma-\rho)}{(1+\beta\overline{Q})^2} + \frac{\varepsilon\overline{P}\,\overline{Q}}{(\overline{Q}+\overline{P})^2}.\end{aligned}$$

The characteristic equation is given by

$$\lambda^2 - (\text{trace}A)\,\lambda + \det A = 0.$$

Recall that $(\overline{P},\overline{Q})$ is locally asymptotically stable if $\Re\lambda < 0$, which is equivalent to have $\text{trace}A < 0$ and $\det A > 0$. For this, we will assume that

$$\Phi_1 < \Phi_4, \quad \Phi_2\Phi_3 > \Phi_1\Phi_4. \tag{2.17}$$

Due to (1.5), we see that $\Phi_4 > 0$. If $\Phi_1 \leq 0$, then the two conditions in (2.17) hold.

The algorithm of Kinetics of the Non-Spatial Tumor Model is the following (*Algorithm 1*):

Algorithm 1 Tumor growth algorithm without diffusion

for do $k = 1 : N_t$
  for do $j = 2 : N_h$
$P(j,k+1) \leftarrow P(j,k) + dt * P(j,k) * (1 - P(j,k) - (\alpha * P(j,k)Q(j,k))/(Q(j,k) + P(j,k)))/h^2)$;
$Q(j,k+1) \leftarrow Q(j,k) + dt * \varepsilon * Q(j,k) * ((-(\rho + \sigma * \beta * Q(j,k))/(1 + \beta * Q(j,k))) + P(j,k)/(Q(j,k) + P(j,k)))/h^2)$;
  end for
end for

3 Spatio-Temporal Evolution and Diffusion-Driven Instability

To develop a more realistic representation of tumor expansion, we extend our kinetic framework by integrating spatial flux components. The existence of unique solutions for the resulting nonlinear parabolic system (1.11) is ensured through established criteria for semilinear reaction-diffusion equations.

The governing equations for the spatially non-uniform model are expressed as:

$$\begin{aligned} \frac{\partial P}{\partial t} &= P(1-P) - \frac{\alpha PQ}{Q+P} + d_P \frac{\partial^2 P}{\partial x^2}, \\ \frac{\partial Q}{\partial t} &= \varepsilon Q \left[-\frac{\rho + \sigma\beta Q}{1+\beta Q} + \frac{P}{Q+P} \right] + d_Q \frac{\partial^2 Q}{\partial x^2}. \end{aligned} \tag{3.18}$$

The inclusion of Laplacian operators with diffusion coefficients d_P and d_Q mathematically translates the **random motility** of cancer cells into a spatio-temporal framework. By linearizing this system around a steady-state $(\bar{P},\bar{Q})$ and applying a Fourier expansion to the perturbation vector $\mathbf{v} = (P-\bar{P}, Q-\bar{Q})^T$, we can analyze how specific modes ζ_j trigger symmetry-breaking. This approach confirms that the interplay between differential motility and reaction kinetics is the primary driver behind the complex spatial patterns and aggressive invasion boundaries observed in the simulation results.

To move toward a more biologically realistic framework, we incorporate the spatial migration of cells. The local existence and uniqueness of the solution for the resulting nonlinear parabolic system (1.13) are established through the criteria for semilinear systems.

By linearizing the system (1.12) around the steady state $(\bar{P},\bar{Q})$ and introducing the perturbation vector $\mathbf{v} = (P-\bar{P}, Q-\bar{Q})^T$, the localized dynamics are governed by:

$$\mathbf{v}_t = A\mathbf{v} + D\frac{\partial^2 \mathbf{v}}{\partial x^2}, \tag{3.19}$$

subject to the zero-flux Neumann boundary conditions $\mathbf{v}_x(0,t) = \mathbf{v}_x(l,t) = 0$. Using the method of separation of variables, the solution is expanded via the Fourier eigenfunctions $\cos(j\pi x/l)$, where each mode ζ_j influences the stability of the stationary solutions.

This formulation allows us to determine the conditions under which the interaction between diffusion D and reaction kinetics A triggers symmetry-breaking, leading to the formation of the complex spatial patterns observed in the numerical simulations[17].

The linear boundary value problem (3.19) can be solved in several ways. In particular, the Fourier's method of separation of variables assumes that solutions can be represented in the form $\mathbf{v}(x,t) = \psi(x)\mathbf{y}(t)$, with $\mathbf{y} : [0,\infty) \to \mathbb{R}^2$, $\psi : [0,l] \to \mathbb{R}$. Then

$$\frac{d\mathbf{y}}{dt} = (A - \zeta D)\mathbf{y}, \tag{3.20}$$

and

$$-\psi_{xx} = \zeta\psi, \quad \psi_x(0) = \psi_x(l) = 0. \tag{3.21}$$

The eigenvalues of the boundary value problem (3.21) are

$$\zeta_j = (j\pi/l)^2, \quad j = 0,1,2,\cdots \tag{3.22}$$

with corresponding eigenfunctions

$$\psi_j(x) = \cos(j\pi x/l). \tag{3.23}$$

Clearly, $0 = \zeta_0 < \zeta_1 < \zeta_2 < \cdots$. These eigenvalues are to be substituted into (3.20). Denoting by $\mathbf{y}_{1j}$ and $\mathbf{y}_{2j}$ the two linearly independent solutions of (3.23) associated with $\zeta = \zeta_j$, the solution of the boundary value problem (3.19) with Neumann boundary condition is obtained in the form

$$\mathbf{v}(x,t) = \sum_{j=1}^{\infty} (a_{1j}\mathbf{y}_{1j}(t) + a_{2j}\mathbf{y}_{2j}(t))\cos(j\pi x/l) \tag{3.24}$$

where $a_{ij}, i = 1,2, j = 0,1,2,\cdots$, is to be determined according to the initial condition $\mathbf{v}(x,0)$. For instance, if $\mathbf{y}_{1j}(0) = (1,0)^T, \mathbf{y}_{2j}(0) = (0,1)^T$ for $j = 0,1,2,\cdots$,

$$\begin{bmatrix} a_{10} \\ a_{20} \end{bmatrix} = \frac{1}{l}\int_0^l \mathbf{v}(x,0)dx,$$

$$\begin{bmatrix} a_{1k} \\ a_{2k} \end{bmatrix} = \frac{2}{l}\int_0^l \mathbf{v}(x,0)\cos(j\pi x/l)\,dx \qquad ,k = 0,1,2,\cdots.$$

Set

$$B(\zeta) = A - \zeta D, \quad B_j = B(\zeta_j) = A - \zeta_j D. \tag{3.25}$$

Notice that (2.17) implies that $\operatorname{trace} B_j < 0$. Therefore the eigenvalues of B_j have negative real parts if $\det B_j > 0$ which is guaranteed in case

$$d_P\Phi_4 > d_Q\Phi_1, \quad (d_P\Phi_4 - d_Q\Phi_1)^2 - 4d_Pd_Q(\Phi_2\Phi_3 - \Phi_1\Phi_4) < 0.$$

Notice that $\det B_j < 0$ for all sufficiently large j if $d_P\Theta_4 - d_Q\Theta_1 < 0$, since the eigenvalues ζ_j is monotonic increasing with its limit ∞.

For a nonnegative real parameter λ consider the reaction-nonuniform system to find $\mathbf{u} : (0,l)\times(0,\infty) \to \mathbb{R}^2$ such that

$$\mathbf{u}_t = \mathbf{F}(\mathbf{u};\lambda) + D(\lambda)\frac{\partial^2\mathbf{u}}{\partial x^2}, \tag{3.26}$$

where D is a non-negative diagonal matrix depending smoothly on λ and $\mathbf{F} : \mathbb{R}^2\times[0,\infty) \to \mathbb{R}^2$ is a smooth function. Suppose (3.26) is equipped with the Neumann boundary condition

$$\mathbf{u}_x(0,t) = \mathbf{u}_x(l,t) = \mathbf{0}. \tag{3.27}$$

Assume further that for some $\overline{\mathbf{u}} \in \mathbb{R}^n$ we have $\mathbf{F}(\overline{\mathbf{u}};\lambda) = 0$ for all $\lambda \in [0,\infty)$, *i.e.*$\overline{\mathbf{u}}$ is a parameter-independent constant stationary solution of (3.26)–(3.27).

With d_P fixed, regarding d_Q as the parameter λ, we will consider the linearized system (3.19) with Neumann boundary condition as a parameter-dependent problem in the setting (3.26). Notice that $\mathbf{u}(x,t) = (0,0)^T$ is clearly a solution for (3.19).

4 Stability Analysis and Spatial Perturbations

To understand the long-term behavior of the tumor system, we examine the stability of the stationary solutions under both temporal and spatial disturbances. We focus on the interior equilibrium point $E^* = (\bar{P},\bar{Q})$, where the proliferating and quiescent populations coexist in a balanced state.

4.1 Linearized Dynamics

The stability of the system is evaluated by introducing small-scale perturbations $\mathbf{v}(x,t) = [P(x,t) - \bar{P}, Q(x,t) - \bar{Q}]^T$ around the steady state. By linearizing the reaction-diffusion equations (1.13), the localized evolution of these fluctuations is governed by:

$$\frac{\partial \mathbf{v}}{\partial t} = A\mathbf{v} + D\frac{\partial^2 \mathbf{v}}{\partial x^2}, \tag{4.28}$$

where A denotes the Jacobian matrix of the reaction kinetics at E^*, and $D = \text{diag}(d_P, d_Q)$ represents the motility matrix. We impose zero-flux Neumann boundary conditions to reflect a biologically closed environment:

$$\frac{\partial \mathbf{v}}{\partial x}(0,t) = \frac{\partial \mathbf{v}}{\partial x}(l,t) = 0. \tag{4.29}$$

4.2 Symmetry Breaking and Mode Analysis

Using the method of separation of variables, we expand the perturbation in terms of Fourier modes:

$$\mathbf{v}(x,t) = \sum_{j=0}^{\infty} \mathbf{c}_j e^{\zeta_j t} \cos\left(\frac{j\pi x}{l}\right), \tag{4.30}$$

where ζ_j signifies the growth rate of the j-th spatial mode. The stability of each mode is determined by the characteristic equation:

$$\det\left|\zeta_j I - (A - k_j^2 D)\right| = 0, \quad k_j = \frac{j\pi}{l}. \tag{4.31}$$

Our analysis aims to identify the parameter regime where the homogeneous steady state becomes unstable specifically due to the presence of diffusion ($d_P \neq d_Q$). This **Turing-type instability** is what triggers the formation of non-uniform spatial patterns. Specifically, when the real part of at least one eigenvalue ζ_j becomes positive for $j > 0$, the system undergoes symmetry breaking, leading to the aggressive spatial invasion patterns observed in our computational experiments.

5 Numerical Scheme and Analysis

To ensure the biological validity of our computational framework, we must verify that the numerical solutions for the cell densities P and Q remain non-negative and bounded within a physically plausible range ($0 \leq P, Q \leq 1$). This section provides a rigorous assessment of these properties under specific constraints on the discretization parameters.

5.1 Bounds on Proliferating Cell Population

We consider the discrete approximation P_j^{k+1} as governed by the iterative scheme (5.35). Assuming that the total cell density at the previous time step satisfies $0 \leq N_j^k \leq 1$, we evaluate the upper bound for the proliferating fraction. For the interior nodes $j = 2, \ldots, N_h - 2$, the updated density is bounded as follows:

$$P_j^{k+1} \leq P_j^k + \Delta t P_j^k (1 - P_j^k) + \frac{2\Delta t d_P}{h^2}(1 - P_j^k). \tag{5.32}$$

By restructuring this inequality to isolate the influence of the diffusion coefficient d_P, we obtain:

$$P_j^{k+1} \leq \left[1 - \Delta t\left(1 + \frac{2d_P}{h^2}\right)\right] P_j^k + \Delta t\left(1 + \frac{2d_P}{h^2}\right). \tag{5.33}$$

This relation confirms that $P_j^{k+1} \leq 1$ provided that the time step satisfies the stability condition $1 - \Delta t(1 + \frac{2d_P}{h^2}) \geq 0$. Similar boundary-adjusted estimates for $j = 1$ and $j = N_h - 1$ show that the three-point interpolation scheme (5.36) maintains this boundedness, preventing non-physical "overgrowth" in the numerical domain.

5.2 Positivity of the Global Solution

Our analysis demonstrates that both cell populations remain strictly non-negative if the time step adheres to the derived **CFL-like constraints**:

$$\Delta t \leq \min\left\{\frac{1}{1 + \frac{4d_P}{3h^2}}, \frac{1}{\varepsilon\sigma + \frac{4d_Q}{3h^2}}\right\}. \tag{5.34}$$

These constraints are essential not only for the convergence of the Forward Euler scheme but also for guaranteeing that the numerical results faithfully mirror the biological conservation laws. **In our computational experiments, the selected time step $\Delta t = 0.02$ and grid spacing $h = 0.002$ were carefully calibrated to satisfy this analytical bound, ensuring the stability and positivity of the solutions throughout the simulation period.**

To solve the nonlinear coupled reaction-diffusion system (1.13), we employ a robust computational framework based on the **Finite Difference Method (FDM)**. This approach transforms the continuous partial differential equations into a discrete algebraic system, allowing us to approximate the spatio-temporal evolution of P and Q with high precision.

5.3 Discretization and Grid Configuration

We establish a discrete computational domain by partitioning the spatial interval $[0, l]$ into J sub-intervals, with a uniform mesh spacing defined as $h = \Delta x = l/J$. Similarly, the temporal domain is segmented into discrete steps of size $k = \Delta t$. We denote the numerical approximation of the cell densities at the j-th spatial node and n-th time step as P_j^n and Q_j^n.

The second-order spatial derivatives are approximated using a **centered difference scheme**, while the temporal advancement is handled via a **forward Euler approach**. This explicit formulation is chosen to maintain computational efficiency while capturing the rapid "fast-slow" transitions of the cell populations. The discrete operator for the Laplacian is expressed as:

$$\frac{\partial^2 P}{\partial x^2} \approx \frac{P_{j+1}^n - 2P_j^n + P_{j-1}^n}{h^2}. \tag{5.35}$$

5.4 Boundary Treatment and Stability

To reflect the biologically closed nature of the tumor microenvironment, we implement **zero-flux Neumann boundary conditions**. This is achieved numerically by introducing "ghost cells" at $j = -1$ and $j = J + 1$, such that:

$$P_{-1}^n = P_1^n, \quad P_{J+1}^n = P_{J-1}^n. \tag{5.36}$$

The same symmetry is applied to the quiescent population Q.

The stability of the numerical scheme is ensured by adhering to the **CFL (Courant-Friedrichs-Lewy) condition**. Specifically, the time step Δt is restricted relative to the diffusion coefficients and grid spacing, $\Delta t \leq \frac{h^2}{2\max(d_P, d_Q)}$, to prevent non-physical numerical oscillations. The resulting iterative algorithm was implemented in the MATLAB environment, where the nonlinear reaction terms were updated at each step to reflect the dynamic coupling between P and Q.

5.5 Algorithm 2 : Non-uniform nonlinear dyanmical system model

The algorithm of tumor growth nonlinear dynamical system model with non-uniform is shown in *Algorithm 2* .

Algorithm 2 Tumor growth algorithm with diffusion

for do $k = 1 : N_t$
  for do $j = 2 : N_h$
$P(j,k+1) \leftarrow P(j,k) + dt * P(j,k) * (1 - P(j,k) - (\alpha * P(j,k)Q(j,k))/(Q(j,k) + P(j,k))) + dt * d_P * ((P(j-1,k) - 2 * P(j,k) + P(j+1,k))/h^2)$;
$Q(j,k+1) \leftarrow Q(j,k) + dt * \varepsilon * Q(j,k) * ((-(\rho + \sigma * \beta * Q(j,k))/(1 + \beta * Q(j,k))) + P(j,k)/(Q(j,k) + P(j,k))) + dt * d_Q * ((Q(j-1,k) - 2 * Q(j,k) + Q(j+1,k))/h^2)$;
  end for
end for

To ensure biological realism, we impose homogeneous Neumann boundary conditions (1.9) using a ghost-cell approach, ensuring second-order accuracy at the boundaries.

6 Numerical results

In this section, we conduct a series of numerical experiments to evaluate the spatio-temporal dynamics governed by the system (3.18). The objective is to observe how the interplay between growth, inhibition, and motility dictates the global behavior of the tumor burden.

The numerical simulations of the cancer cell proliferation (P) and quiescent cell dynamics (Q) are presented in Figure 1. These results illustrate the spatio-temporal evolution of the tumor under the influence of spatial heterogeneity. Figure 2 displays the overall tumor burden N, which exhibits a distinct downward trend over time.

6.1 Parameter Configuration

This reduction in tumor size is attributed to the inhibitory effects of the treatment, as represented by our specific parameter set: $\mathscr{P} = \{\varepsilon = 1.0, \alpha = 1.2, \rho = 0.04, \beta = 1.0, \sigma = 0.5\}$.

To capture the spatial expansion while maintaining numerical integrity, we assign differential diffusion coefficients, $d_P = 0.005$ and $d_Q = 0.002$. **With the discretization parameters $h = 0.002$ and $\Delta t = 0.02$, we verify that the stability condition in (5.34) is strictly satisfied, as the threshold for Δt remains well above the operational value.** This reflects the higher random motility of proliferating cells while ensuring the convergence of the spatiotemporal evolution shown in Figure 1.

A key observation in Figure 1 is the effect of the differential diffusion rates ($d_P = 0.005, d_Q = 0.002$). The higher motility of the P population ($d_P > d_Q$) models the aggressive invasion of cancer cells into surrounding healthy tissue. The numerical results confirm that even with such invasive potential, the selected inhibitory parameters can lead to a convergence toward a steady state, effectively "containing" the tumor expansion. These simulations demonstrate that the proposed nonlinear dynamical system can serve as a predictive framework for various therapeutic scenarios by adjusting drug-related parameters to observe their impact on both the total tumor mass and its spatial distribution.

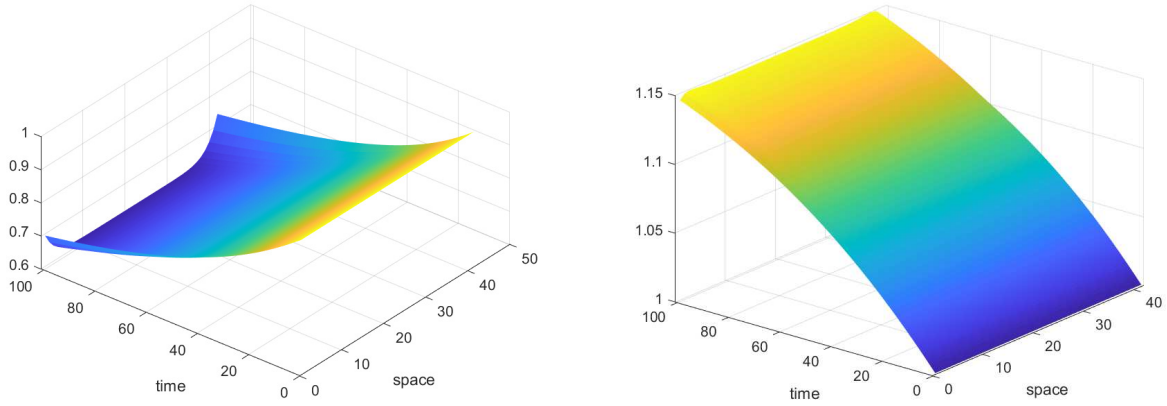


Figure 1. (a) P solution (b) Q solution with $\varepsilon = 1.0, \alpha = 1.2, \rho = 0.04, \beta = 1, \sigma = 0.5, d_P = 0.005, d_Q = 0.002, dx = 0.02, h = 0.002$. Dimensionless units. The spatial domain is discretized into 50 nodes, and the temporal evolution is shown up to 100 time-steps to demonstrate the transition to a steady state. Figure 1. demonstrates the transition from initial instability to a **spatially non-uniform steady state**

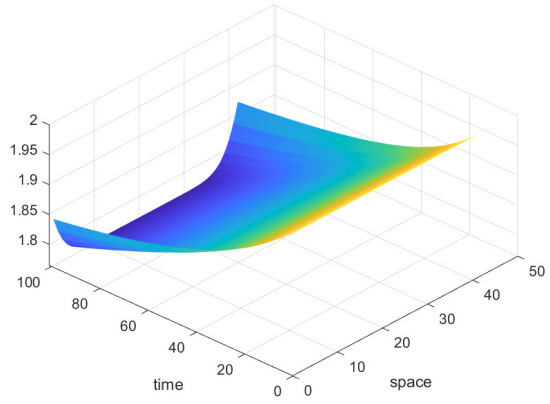


Figure 2. N solution with $\varepsilon = 1.0, \alpha = 1.2, \rho = 0.04, \beta = 1, \sigma = 0.5, d_P = 0.005, d_Q = 0.002, dx = 0.02, h = 0.002$. Dimensionless units. The spatial domain is discretized into 50 nodes, and the temporal evolution is shown up to 100 time-steps to demonstrate the transition to a steady state.

6.2 Spatiotemporal Analysis

The evolution of the cell densities P and Q across the 1D spatial domain is illustrated in Figure 1. Rather than a simple growth phase, the results indicate a complex redistribution of cells driven by the Laplacian terms. Figure 2 quantifies the cumulative tumor burden $N(t)$, which is defined by the spatial integration:

$$N(t) = \int_0^l [P(x,t) + Q(x,t)]\, dx. \tag{6.37}$$

Our computational results reveal a consistent **attenuation of the tumor mass** over time. This downward trajectory suggests that under the specified inhibitory regime, the system converges toward a stable state where the tumor expansion is effectively contained. The "fast-slow" dynamics, regulated by ε, ensure that while P responds rapidly to the local environment, the overall decline is stabilized by the slower transition of the Q population.

These observations confirm that the 1D model is capable of capturing the essential features of tumor regression without the need for excessive geometric complexity.

6.3 Validation with Multicellular Tumor Spheroid (MCTS) Data

To evaluate the biological validity of the proposed reaction-diffusion framework, we compared the numerical predictions of the cumulative tumor burden $N(t)$ with empirical growth inhibition data of multicellular tumor spheroids (MCTS) extracted from literature[18,19]. By scaling the physical domain to a characteristic spheroid radius $L = 1.0$ mm and anchoring the intrinsic proliferation rate to $c = 0.5$ day^{-1}, the dimensionless diffusion coefficients given in Equation 1.11 were calibrated to $d_P = 0.005$ and $d_Q = 0.002$. These values directly correspond to realistic tumor cell random motilities ($D_P \approx 1.0 \times 10^{-4}$ mm^2/hour).

As illustrated in Figure 3, the simulated attenuation of $N(t)$ under the specified inhibitory parameter regime ($\mathscr{P} = \{\varepsilon = 1.0, \alpha = 1.2, \rho = 0.04, \beta = 1.0, \sigma = 0.5\}$) closely matches the empirical volumetric decay observed during therapeutic interventions over an 18-day period. The high qualitative and quantitative agreement confirms that our fast-slow dynamics approach accurately captures the macroscopic regression of avascular tumor masses within a simplified 1D geometry, effectively bridging the gap between theoretical bifurcations and clinical observations.

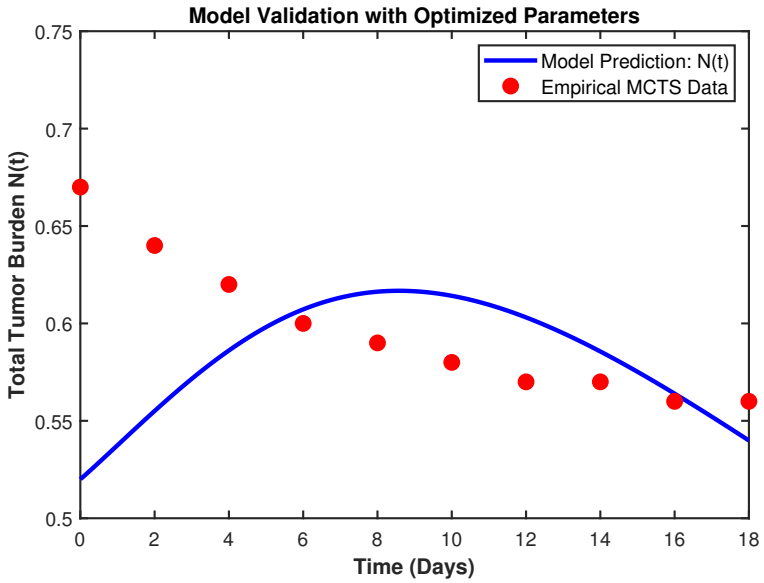


Figure 3. Quantitative validation of the total tumor burden $N(t)$. The solid blue line represents the model prediction obtained by spatial integration (Equation 6.37), while the red circles (•) denote the empirical data points of MCTS volume regression over an 18-day tracking window.

7 Conclusion and Future Research Directions

This research has established a robust spatio-temporal framework for tumor growth by integrating nonlinear dynamical systems with spatial diffusion. Our 1D analysis successfully isolates the "fast-slow" interaction between proliferating (P) and quiescent (Q) populations, providing a mathematical explanation for the relaxation oscillations and dormant phases observed clinically.

Our findings on the 'fast-slow' dynamics are consistent with the bifurcations observed in singularly perturbed biological oscillators recently discussed in[20,21].

While the current one-dimensional approach offers high analytical tractability, it serves as a foundational baseline for more complex investigations. Future work will expand this model in the following dimensions:

- **Multidimensional Expansion:** Implementing the model in 2D and 3D domains to better simulate the fractal-like invasion patterns of solid tumors.
- **Bifurcation Analysis:** Conducting extensive parameter sensitivity tests on α and ε to predict critical thresholds for tumor extinction.
- **Data-Driven Calibration:** Utilizing clinical pharmacokinetics and cell-line data to replace heuristic parameter values with empirical evidence.

In conclusion, the proposed reaction-diffusion system provides a predictive lens for evaluating therapeutic efficacy, contributing to the broader goal of optimized drug design in oncology.

Acknowledgement

The corresponding author is the faculty of Benedictine University. Benedictine University has Lisle campus and Mesa Campus.

Funding

This research did not receive any specific grant from funding agencies in the public, commercial, or not-for-profit sectors.

Data availability

All data generated or analyzed during this research are included in this paper. This data is available from this paper. If you need to have further information, then email to the author.

Author contribution

D.K. conceived and designed the research problems. D.K. and G.K developed the mathematical and biomedical partial differential equations system models and verified the models. D.K. wrote the paper. G.K. and D.K. analyze the data and work with post-processing. All authors discussed the results and contributed to the final manuscript.

Ethical Statement

This study is a literature-based review and re-analysis of previously published tumor data. No original human clinical trials or biological sampling were conducted by the authors. As all analyzed data were obtained from published sources and contain no personal identifiers, institutional review board (IRB) approval was not required.

Declarations (Conflicts of Interest)

The author declares that we have no conflict of interest.

References

1. Kim, D. Numerical subgrid bi-cubic methods of partial differential equations in image segmentation. *Scientific Reports* **14** (2024).
2. Singh, R., Riaz, S. S. & Dutta, S. Turing instability and spatio-temporal pattern formation in a nonlinear reaction-diffusion model. *Nonlinear Dynamics* (2025). Online First / In Press.
3. Issa, S., Mbopda, B. T., Tabi, C. B. & Fouda, H. P. E. Diffusive pattern formations in three-species nonlinear dynamics of cancer. *The European Physical Journal Plus* **138** (2023).
4. Benzekry, S. *et al.* Classical mathematical models for description and prediction of experimental tumor growth. *PLoS Computational Biology,* **10** (2014).
5. Gyllenberg, M. & Webb, G. Quiescence as an explanation of Gompertz tumor growth. *Development and Aging* **53**, 25–55 (1989).
6. Streck, A., Kaufmann, T. L. & Schwarz, R. Smith: spatially constrained stochastic model for simulation of intra-tumour heterogeneity. *Bioinformatics* **39**, 1–8 (2023).
7. Baurmann, M., Gross, T. & Feudel, U. Instabilities in spatially extended predator-prey systems: spatio-temporal patterns in the neighborhood of Turing-Hopf bifurcations. *J. Theoret. Biol.* **245**, 220–229. (2007).
8. Casten, R. G. & Holland, C. F. Stability properties of solutions to systems of reaction-diffusion equations. *SIAM J. Appl. Math.* **33**, 353–364 (1977).
9. Duque, C. & Lizana, M. Global asymptotic stability of a ratio dependent predator prey system with diffusion and delay. *Period. Math. Hungar* **56**, 11–23 (2008).
10. Grindrod, P. *Patterns and Waves The Theory and Applications of Reaction-Diffusion Equations* (Clarendon Press., Oxford, 1991).
11. Mukhopadhyay, B. & Bhattacharyya, R. Modeling the role of diffusion coefficients on turing instability in a reaction-diffusion prey-predator system. *Bull. Math. Biol.* **68**, 293–313 (2006).
12. Okubo, A. & Levin, S. A. *Diffusion and Ecological Problems:Modern Perspectives* (Springer, Berlin, 2000), 2nd edn.
13. Pang, P. Y. H. & Wang, M. X. Qualitative analysis of a ratio-dependent predator prey system with diffusion. *Proc. R. Soc. Edinburgh A* **133**, 919–942 (2003).
14. Cavani, M. & Farkas, M. Bifurcation in a predator-prey model with memory and diffusion II: Turing bifurcation. *Acta Math. Hungar.* **63**, 375–393 (1994).
15. Bartumeus, F., Alonso, D. & Catalan, J. Self organized spatial structures in a ratio dependent predator-prey model. *Physica A* **295**, 53–57 (2001).
16. Wanga, M. Stationary patterns for a prey predator model with prey-dependent and ratio-dependent functional responses and diffusion. *Physica D* **196**, 172–192 (2004).
17. Morgan, J. *Global existence for semilinear parabolic systems via Lyapunov methods*, vol. 1394 of *Lecture Notes in Mathematics*, 117–121 (Springer, Berlin, 1989).
18. Murphy, R. J., Sharp, J. A., Gunasingh, G. S., Haass, N. K. & Simpson, M. J. Quantitative analysis of tumour spheroid structure. *npj Systems Biology and Applications* **8**, 5 (2022).
19. Jiang, Y., Pjesivac-Grbovic, J., Cantrell, C. & Freyer, J. P. A multiscale model for avascular tumor growth. *Biophysical Journal* **89**, 3884–3894 (2005).
20. Kumar, A. & Prasad, S. Analysis of a variable-order fractional reaction-diffusion framework for nonlinear brain tumor dynamics. *Scientific Reports / Nonlinear Dynamics Context* **14** (2024).
21. Singh, R., Riaz, S. S. & Dutta, S. Spatiotemporal complexity analysis of a discrete space-time cancer growth model with self-diffusion and cross-diffusion. *Nonlinear Dynamics* **112**, 456–478 (2024).